IEEE Access
Multidisciplinary | Rapid Review | Open Access Journal

Received August 25, 2020, accepted October 1, 2020, date of publication October 15, 2020, date of current version October 28, 2020.

Digital Object Identifier 10.1109/ACCESS.2020.3031446

Mitigating Power Fluctuations for Energy Storage in Wind Energy Conversion System Using Supercapacitors

IRFAN HUSSAIN PANHWAR[1], KAFEEL AHMED[2], (Member, IEEE), MEHDI SEYEDMAHMOUDIAN[2], (Member, IEEE), ALEX STOJCEVSKI[2], (Senior Member, IEEE), BEN HORAN[3], (Member, IEEE), SAAD MEKHILEF[2,4], (Senior Member, IEEE), ASIM ASLAM[1], AND MARYAM ASGHAR[1], (Member, IEEE)

[1]Electrical Engineering Department, DHA Suffa University, Karachi 75500, Pakistan
[2]School of Software and Electrical Engineering, Swinburne University of Technology, Melbourne, VIC 3122, Australia
[3]School of Engineering, Deakin University, Geelong, VIC 3216, Australia
[4]Power Electronics and Renewable Energy Research Laboratory, Department of Electrical Engineering, University of Malaya, Kuala Lumpur 50603, Malaysia

Corresponding authors: Irfan Hussain Panhwar (irfan.hussain@dsu.edu.pk) and Kafeel Ahmed (kahmed@swin.edu.au)

ABSTRACT The world is rapidly shifting to green power resources due to inevitable growing energy needs and increasing environmental concerns. However, the irregular production capacity of renewable energy resources requires additional components in the system for conditioning power quality and to make them a sustainable solution. It imperatively needs an energy storage system, which is crucial for the wind energy conversion system (WECS) to maintain a smooth power supply to loads. However, voltage fluctuations from the wind turbine generator, which are caused by the turbulent nature of wind speed, pose disruptions to the DC charge controller of a battery, and affects battery life. To deal with power fluctuations of the wind turbine generator, this study proposes a WECS that integrates a supercapacitor before the stages of the DC charge controller and the energy storage device. Given that batteries have transient charging and discharging characteristics, a test bench is developed to analyze their patterns during the charging/discharging cycles. The DC charge controller in the proposed WECS is designed to operate in the constant current mode as well as constant voltage mode depending on the state of charge of the battery. The simulations and experiments associated with the performance of WECS with a hybrid energy storage system and conventional system are carried out and presented to substantiate the assertion. To validate the proposed idea, the performance of the WECS and improvement in battery life are examined through the charging pattern of battery before and after the integration of a supercapacitor. The behavior of wind turbine generator variables due to the integration of supercapacitor in WECS is analyzed and discussed in detail. A prototype of WECS combined with an arrangement of a supercapacitor (500 F, 2.7 Vdc) module is built and tested. The simulation and experimental results indicating the impact of the integration of supercapacitor in WECS are presented.

INDEX TERMS Batteries, DC-DC power converters, energy storage, microgrids, supercapacitors, smart grids, wind energy, wind energy integration.

I. INTRODUCTION

Energy is an important resource in the world today. Countries worldwide are shifting toward renewable energy sources for the generation of electric power. Hence, the concept of the microgrid (MG) has been introduced. A MG system is an off-grid or grid-connected energy system that can work independently or collaboratively with other MGs [1]. A MG system can provide electric power either from a single source or multiple sources, such as wind and solar energy [2]. In most MG systems based on wind energy conversion systems (WECS), adding an energy storage device in the system is necessary [3]. Owing to its highly variable nature, wind power is unreliable for the grid system and occasionally can

The associate editor coordinating the review of this manuscript and approving it for publication was Eklas Hossain.

lead to failures of a power system. This limitation becomes a more critical issue for remote off-grid systems. Moreover, wind power generation needs to fulfill grid codes for synchronization. For this reason, WECS need to absorb power and voltage fluctuations and to regulate injected power.

Energy storage systems (ESS) play a significant role in WECS by controlling wind power plant output and providing auxiliary services to the power system, thus increasing utilization of wind power in the system [4]. The standard choice for the energy storage buffer in a MG is lead–acid batteries [5]. However, lead–acid batteries as an energy storage buffer have low power density and a high rate of charge and discharge [6]. As a result, their usage causes immoderate stress on battery cells under fast load variations, which causes a high number of charge and discharge cycles. For this reason, the lifetime of a battery is reduced significantly. In contrast, a supercapacitor has high power density and quick response to load variations [7]. Owing to the rapid charge and discharge rate of supercapacitors, ESS based on supercapacitor is ideal for preventing power fluctuations in renewable energy conversion systems [8]. However, a supercapacitor alone cannot be used as an energy storage device wherein several hundred to thousand amperes of current is supplied for a short period [7]. Supercapacitors have eliminated the energy and power gap between electrolytic capacitors and batteries. The energy capacity of a supercapacitor is typically a hundred times more than that of an electrolytic capacitor of the same size. A supercapacitor has a wide range of operating temperatures, and it holds high power density of approximately 10 kW/kg, which is more than that of a battery. It has a long lifecycle of around 500,000 cycles. A supercapacitor can store charge without any chemical reaction. Thus, it can charge and discharge at a much faster rate in a matter of a few seconds. By contrast, lead–acid batteries are electrochemical devices that convert chemical energy into electrical energy through a reduction and oxidation process called ''redox'' [9]. As a result of the chemical reaction, the charging process is slow. Lead–acid batteries provide energy to the rated load for an extended period or high power for short durations, depending on the intended application [10]. Typically, the energy density of a battery is $10-100$ kW/kg, and the charge cycles are approximately 1,000 cycles. Thus, a battery cannot sustain a high number of charge/discharge cycles in MGs [7], [8]. Under extreme load variations, batteries cannot respond immediately and remain under high stress, which reduces the lifetime of a battery.

Many research articles have been published about WECS that use hybrid energy storage systems (HESS) consisting of a battery and a supercapacitor [10]–[12]. Verboomen *et al.* [10] have proposed a model for fast power fluctuation caused by demand side load, which puts stress on batteries. They proposed a battery for energy requirements and a supercapacitor to fulfill power needs. No battery charging/ discharging is discussed during wind turbine power fluctuations. Gee and Dunn [12] and [13] have proposed a control methodology that quantified battery lifetime by adding a supercapacitor. Kollimalla *et al.* [6] have proposed a control strategy for batteries and supercapacitors by decoupling low and high frequency component by utilizing error component of battery current to control the supercapacitor. The control strategies presented in [6], [12]–[14] are based on control of the low and high frequency component, while considering demand side load. However, the impacts of power fluctuations on batteries and an investigation on battery life damage have not been covered yet. Ayodele *et al.* [15] proposes the use of supercapacitor in photovoltaic (PV) system to improve battery lifetime. The analysis was done using MATLAB, and battery lifetime was estimated using Schiffer's technique. The impact of a battery–supercapacitor HESS and its different topologies in standalone DC MGs have been discussed in [16]–[18] have presented the analysis of ESS in renewable energy sources for voltage regulation.

The battery–supercapacitor HESS introduces technical benefits of high power density by maintaining the same energy density as those of conventional battery systems. However, substantial cost is added due to the addition of supercapacitors. Comparing different ESS is difficult because of their variances in technical specifications and application diversity. Thus, Table 1 shows a comparison of their characteristics including energy density, power density, lifetime, financial benefits, and other aspects. When energy storage devices are compared in terms of their lifetime, the key performance indicators reveal that hybrid energy storage will reduce the overall cost of a system. The stable power from hybrid energy storage will reduce the impacts of frequent transients of turbulent wind energy source on the system, thereby increasing the life of energy storage device and other associated power electronic components. Thus, the hybrid energy storage not only maintains stable power but also increases the lifetime of the overall system.

This paper proposes a wind energy conversion system that involves a HESS composed of supercapacitors and batteries. It emphasises the assessment of impact due to power fluctuations of WECS on battery life during a charging cycle. Furthermore, the study signifies improvements in battery charging characteristics by integrating the HESS in WECS compared with the conventional system. Section II describes the structure of the proposed WECS. Section III presents the design of the charge controller and its control algorithm. Section IV details the charging/discharging characteristics of a battery. Section V covers the selection of supercapacitor and its sizing principle. Section VI discusses the simulation and experimental study of the proposed system. Finally, Section VII concludes this study.

II. WIND ENERGY CONVERSION SYSTEM

The WECS is composed of mechanical and electrical components. Mechanical components include wind turbine and gearbox. The electrical part consists of the generator, control, and other interconnected devices [23]. The generator is the integral part of a wind turbine, because it is responsible for converting mechanical energy into electrical energy [24].

TABLE 1. Characteristics of different (ESS) devices [16], [19]–[22].

Energy Storage System	Energy Density (Wh/L)	Power Density (W/L)	Response Time (time)	Overall Efficiency (%)	ESS Lifetime (years)	Life Cycles	Energy Capital Cost ($/kWh)
Lead–acid Battery	50–100	10–400	< seconds level	70–90	5–15	500–1,800	200–400
Lithium-ion Battery	200–500	1,500–10,000	< seconds level	80–95	5–15	1,000–20,000	600–2,500
Zinc–bromine Battery	55–65	10–25	< seconds level	65–80	5–10	2,000+	150–1,000
Sodium–sulfur Battery	150–250	140–180	< seconds level	70–90	10–20	2,500–4,500	300–500
Flywheel	20–80	1,000–5,000	< seconds level	90–95	15–20	20,000+	1,000–5,000
Supercapacitor (SC)	10–30	100,000+	< seconds level	90–97	10–30	100,000+	300–2,000
Superconducting Magnetic Energy Storage (SMES)	0.2–6	1,000–4,000	< seconds level	90–98	20+	100,000+	1,000–10,000
Hybrid Energy Storage System (SC + Battery)	141+	30,127+	< seconds level	84–100	5–25	50,000	-

Different types of electrical generators are normally used in wind turbines. In WECS, asynchronous and synchronous generators are generally used, depending on the configuration [25]. Most WECS use a doubly fed induction generator or a permanent magnet synchronous generator. The permanent magnet generator does not require a gear box, because this generator is typically used to charge a battery energy storage through a rectifier [23], [24]. Wind power sources, which are located far from inhabited areas and are capable of small-scale power generation, need to store electrical energy. These power sources form MGs through the addition of energy storage devices in WECS. Energy storage devices are connected to these types of sources either directly, by means of rectifier or DC-DC converters, or by their cascaded combination [26]. Given that the three-phase rectifier converts the AC voltage generated by the wind turbine and the output of the rectifier is irregular DC voltage, a DC-DC converter is used to regulate DC voltage.

The WECS under study is composed of a mimicking converter, supercapacitor, charge controller, and a battery as shown in Figure 1. The mimicking converter represents the wind turbine generator, rectifier and DC-DC converter. The DC supply from the DC-DC converter is fed to charge the supercapacitor. The supercapacitor supplies the stored power to the charge controller to charge the battery. The control

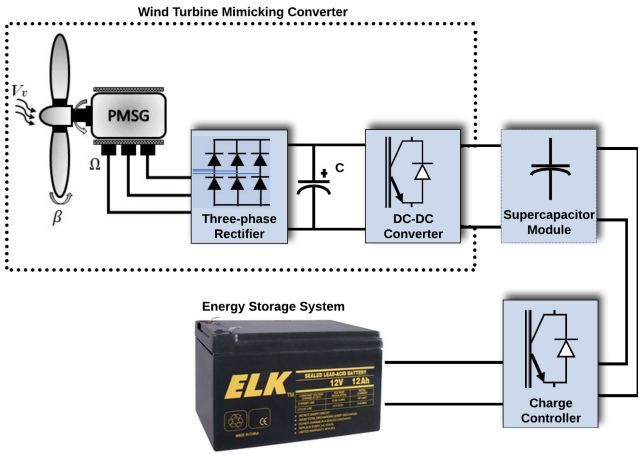

FIGURE 1. Wind Energy Conversion System with proposed HESS.

of the charge controller is designed to operate in constant current/voltage mode. The proposed WECS is designed to operate independently in a single MG or collaboratively with other MGs. The battery voltage (DC) can be fed to the power converter (DC-AC) to supply AC loads.

III. DESIGN AND CONTROL OF DC-DC CONVERTER

DC charge controllers are capable of converting any level of DC to another level, and they play a vital role in the charging of energy storage devices [27], [28]. Batteries are used as energy storage elements in most wind energy systems [29]. The turbulent nature of wind source and short-term load variations cause frequent charging/discharging of batteries, which is a common occurrence in WECS. Frequent charging and discharging increases the number of charge/discharge cycles, thus reducing battery life [13]. Many chargers of lead-acid batteries, which are available in the market, use power dissipating methods for charging, which result in a reduction of battery life [30]. Therefore, charging lead-acid batteries requires a state-of-the-art power converter. The proposed control of the DC charge controller handles power variations by adding a supercapacitor before battery and maintains power supply according to the charging/discharging profile of the specific battery. Thus, the converter control is designed to track the error of current control. Hysteretic current-mode control is applied to maintain the current regulation in the DC-DC converter and to provide excellent performance in operating conditions [13], [31].

A. DESIGN OF CHARGE CONTROLLER

Various PWM controllers are used to control DC-DC converters, DC-AC power inverters, and other voltage control applications. The 16-pin Integrated Circuit UC3525 from *Texas Instruments* is a chip dedicated to converters and battery charging applications [32]. Many topologies of the DC-DC converter can be used for different voltage and power levels. The buck-type DC-DC converter is selected for the charge controller in this study as it has endurance, design symmetry, and power management capability [33]. Figure 2 shows the charge controller and its control.

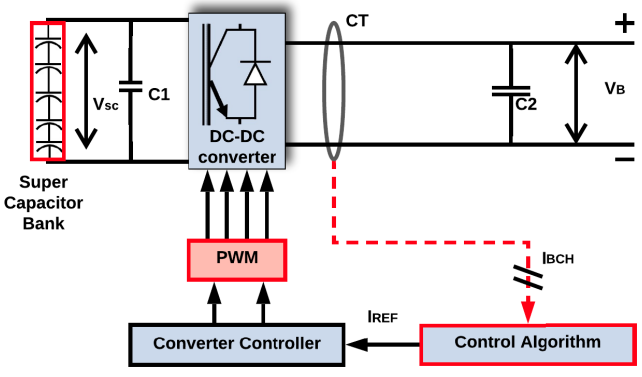

FIGURE 2. DC charge controller and its control mechanism.

The full-bridge charge controller is responsible for providing constant current and voltage output for charging the battery. For this purpose, the built-in error amplifier of the PWM controller continuously senses feedback current (I_F) from the current transducer and matches it with the reference voltage level of the error amplifier to maintain the charging current supplied to the battery (I_{bat}), as shown in Figure 3.

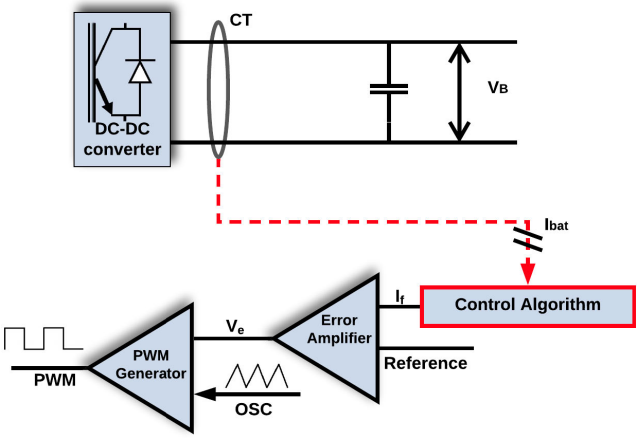

FIGURE 3. Structure of the error amplifier.

The error amplifier results in a command signal to the PWM controller to vary the PWM signals by changing the duty cycle (D) of square-wave pulses [34]. The PWM signals fed to a metal–oxide–semiconductor field-effect transistor (MOSFET) switches from Q1 to Q4 to accomplish the desired current output of the converter. The supercapacitor bank with a variable input of 24 V to 16 V feeds to the charge controller. The control algorithm applied at the charge controller accomplishes the constant DC voltage by sensing feedback from a voltage divider. The control algorithm switches between constant current and voltage mode depending on the SOC of the battery, as illustrated in Figure 4.

The output voltage of the buck converter can be calculated as follows:

$$V_{out} = \frac{1}{1-D} \times V_{in}, \tag{1}$$

where (D) is the duty cycle and (V_{in}) is the input voltage of the converter bridge.

From equation (1), the feedback system appears to only need to change the duty cycle of PWM applied to Q1–Q4 MOSFETs.

B. CONTROL ALGORITHM OF CHARGE CONTROLLER

The charge controller uses the multi-stage charge algorithm for effective charging. The control algorithm should comply with the requirements of the voltage and current of the battery [31]. The SOC of the battery is taken into account to set the references for current and voltage control. This multi-stage charge control algorithm is programmed in a microcontroller, which adjusts the references of current and voltage. This algorithm is executed separately along with the PWM controller.

The multi-stage charge algorithm is represented by a flow chart in Figure 4, in which each charging stage indicates different charging parametric values according to the SOC of the battery. The multi-stage algorithm can be applied in WECS with multiple energy storage devices.

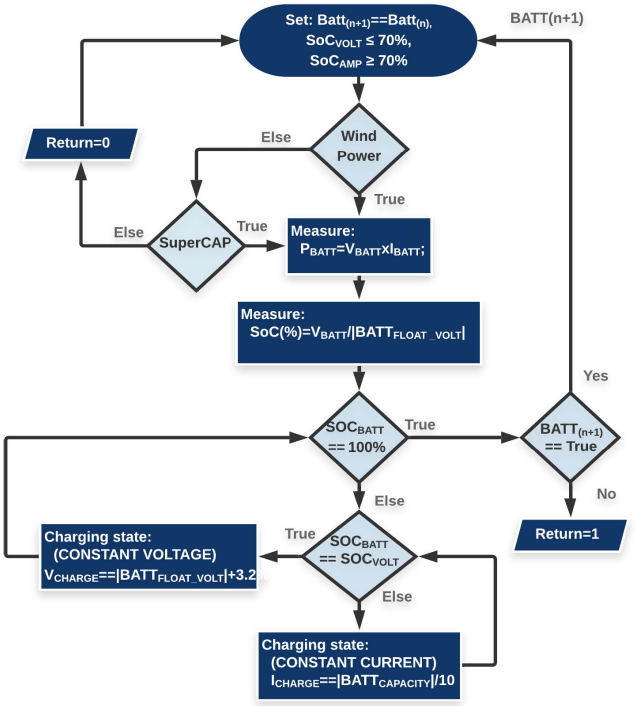

FIGURE 4. Flow Chart of Charge Controller with Constant Current/Voltage Mode.

The transition from one charging mode to another expedites on certain SOC thresholds, specified in the initialization block of the flow chart as SOC_{AMP} (for constant current charging mode) and SOC_{VOLT} (for constant voltage charging mode).

The SOC of the battery is continuously determined through voltage (V_{bat}) and current (I_{bat}). After the computation of SOC, the result is compared with SOC thresholds to decide the optimum charging mode. In the case of multiple energy storage devices, if the first bank is fully charged, then the charger shifts to subsequent energy storage devices. However, if the SOC is less than 100% but higher than the specified transient threshold, then constant voltage mode proceeds, otherwise constant current mode takes place. In either scenario, the battery SOC is repeatedly measured with an inevitable delay to assure the smooth transition of one charging stage to another.

The depth of the discharge (DOD) and SOC are the main parameters of the battery. The DOD indicates how deeply the battery is discharged and it can be represented as follows [34].

$$DOD\,(\%) = \frac{Q_d}{Qrated}\text{X}100, \tag{2}$$

where Q_d is the discharged capacity of the battery, and Q_{rated} is the rated capacity. The measurement unit for both is ampere hour (Ah).

The SOC term is used to describe the remaining energy reserves of the battery in percentage form. The SOC of a fully charged battery is 100% and that of an empty battery is 0%. The SOC of the battery can be written as follows [34], [35].

$$SOC\,(\%) = \frac{Q_{rem}}{Q_{rated}}\text{X}100, \tag{3}$$

where Q_{rem} specifies the remaining capacity of the battery.

IV. CHARGING/DISCHARGING CHARACTERISTICS OF THE BATTERY

The charging/discharging behavior has a significant impact on the lifetime of a battery. The lead–acid battery has main components, including two electrodes, an electrolyte, and terminals. The structure of the electrodes consists of a grid and active materials. The grid provides physical support to the active material and distributes the charging and discharging current [36]. Fundamentally, the chemical reaction occurs in the battery, which converts chemical energy into electrical energy [10]. The electrodes are soaked by electrolyte material that enables ion exchange to conduct electricity. In lead–acid batteries, the discharging process turns electrodes into lead sulphate crystals, whereas the electrolyte (sulphuric acid) is converted into water [33]. The sulphate crystals become a solution and turn into PbO_2 and Pb on the positive and negative electrodes, respectively. The charging method of a battery is an essential factor that affects the lifetime of the battery, and it controls the duration of charging, temperature, and charging status [37]. The charging mechanism should have the ability to protect the battery from under- and overcharge to increase its lifetime. In lead–acid batteries, the charging process leads to the transformation of the sulfuric acid of the electrolyte as follows.

$$SO_4 + 2H^+ = H_2SO_4. \tag{4}$$

The net recharge reaction on both electrodes and the electrolyte is represented by following equation:

$$2PbSO_4 + 2H_2O = PbO_2 + 2H_2SO_4 + Pb. \tag{5}$$

The power flow is shown in equivalent circuit of battery in Figure 5. The battery parameters C_b, V_{cb} represent the lumped capacitance and electromotive force, respectively.

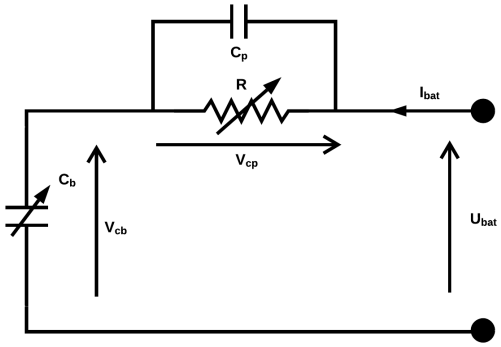

FIGURE 5. Equivalent Circuit for the Battery [34], [38].

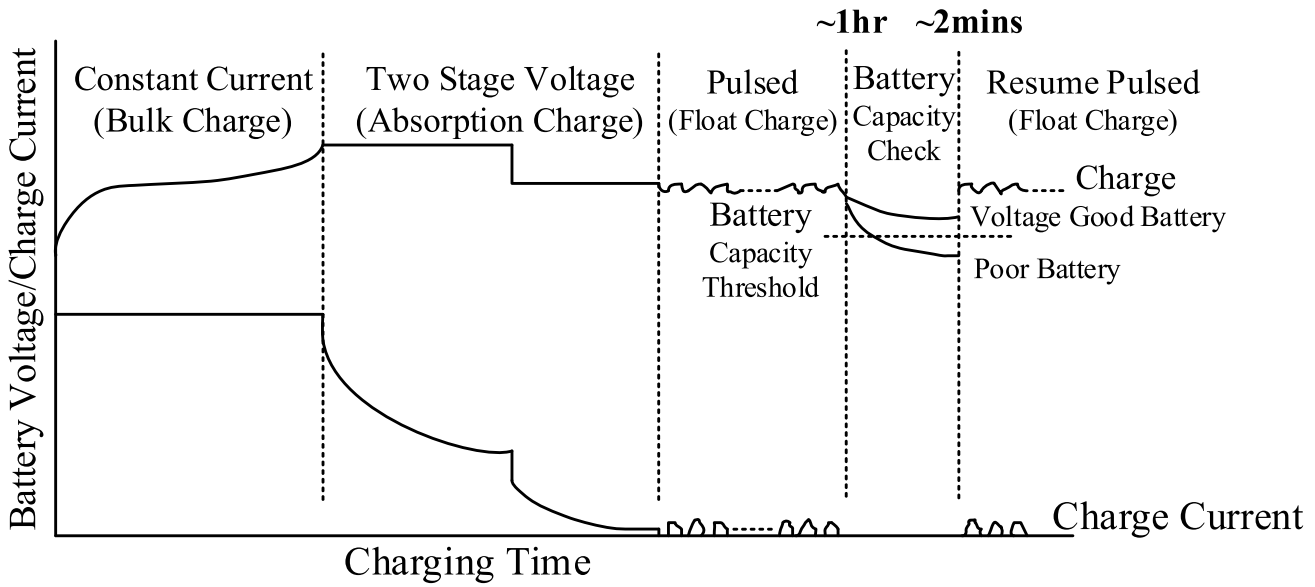

FIGURE 6. Charge Profile of Lead–acid Battery [39].

Whereas, C_p and V_{cp} are the polarization capacitor and polarization voltage, respectively. I_{bat} and U_{bat} are the battery current (amperes) and battery voltage (volts) respectively. To increase the lifetime of the battery, constant current/constant voltage (multistage) charging techniques are considered. In the first part of the multistage charging method, the constant current mode is applied to the battery. At this stage, the current must be limited to a maximum of 0.25 C Amps, which is a quarter of the total battery capacity. For example, if the full battery capacity is 4 Ah, then the charging current should not exceed 1 Amp [39]. Figure 6 shows the typical charge profile of a lead–acid battery. This method is used to reduce charging time, and it requires precise SOC detection of a battery. Constant current is applied until the battery voltage reaches 70%–80% of the upper threshold voltage (UV_{Th}) [9]. In this mode, the battery terminal voltage is continuously monitored until it hits 14.4 V (UV_{Th}) in the case of a 12 V battery. The constant voltage mode is automatically triggered as the battery terminal voltage hits 14.4 V. At this stage, the charging current is monitored. When it drops to 0.05 C Amps, which means 0.2 Amps for a 4 Ah battery, then the battery voltage reduces to 13.65 V. This reduction indicates that the battery has recovered its charge to 70%–80% of its capacity. The remaining 20%–30% is to be charged with lower voltage to prevent overcharging.

V. SELECTION/CHOICE OF SUPERCAPACITOR

A. MODELING OF SUPERCAPACITOR

A supercapacitor supplies energy in the form of an electrostatic field. The energy (E) stored in the supercapacitor is directly related to the square of the applied voltage. This relation is quantified by the following equation [10], [40].

$$E = \frac{1}{2}CV^2 \tag{6}$$

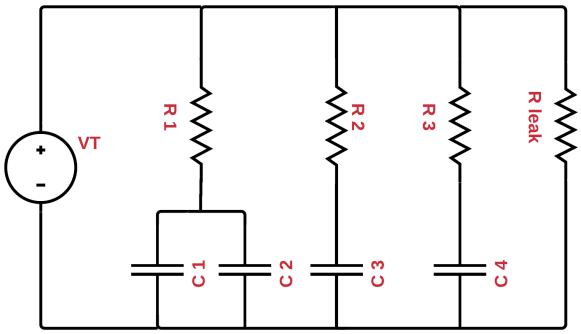

FIGURE 7. Supercapacitor model of Zubieta and Bonert.

The process of energy storage in a supercapacitor is different from that in batteries. Ideally, a supercapacitor is suitable for providing energy in applications where charging/discharging cycles of high current frequently occur in short durations. However, batteries are appropriate for systems with infrequent charging/discharging cycles and take a longer charging/discharging duration than supercapacitors. Combining both into a hybrid form meets the energy and power need in WECS and reduces battery stress, which reflects in the increment in life span. The discharge method of a supercapacitor is governed by the following equation [41].

$$V(t) = V_c\,(0)\,e^{-\frac{t}{R_P C}}, \tag{7}$$

where V_C (0) is the initial voltage of the supercapacitor and R_P and C represent parallel resistance and capacitance, respectively [41]. The supercapacitor model used in this research was presented by Zubieta and Bonert [42]. Figure 7 illustrates the model, which is a simple RC circuit that provides the terminal behavior of a supercapacitor. The three-branch model of supercapacitor charge distribution is developed from the RC circuit configuration.

The resistive component represents the resistivity of active carbon material. The supercapacitor equivalent series resistance (ESR) is modeled by the R_1, R_2, R_3, and R_{leak}; R_{leak} is the self-discharge leakage, and it is modeled by the parallel resistor R_{leak}. The capacitive element C_1, C_2, C_3, and C_4 represent the capacitance between the carbon and electrolyte. The capacitance of the supercapacitor charge depends on the potential difference between carbon and electrolyte material. The ESR and the leakage resistances are accounted for the energy wastage, which lowers the efficiency of the supercapacitor. Owing to the high charge/discharge power levels, the supercapacitor is suitable for energy buffering. However, due to ESR and leakage resistance, some power is consumed, which limits the efficiency to less than 100% [42], [43].

The efficiency (η) of the supercapacitor is the ratio between the useful power (P) and the total power. The total power includes useful power and internally wasted power (P_w). The efficiency of the supercapacitor is represented by the following equation [43].

$$\eta = \frac{P}{P + P_w} \times 100\%, \tag{8}$$

B. SIZING OF SUPERCAPACITOR

The supercapacitor has a limitation to withstand a voltage range of 2.5 V to 2.7 V. Typically, supercapacitors should work in series and parallel combination to achieve high levels of power. The recharging current depends on the value of supercapacitance and internal losses known as leakage resistance. The permissible limits of system variables including current, voltage, charging/discharging time, and power determine the quantity of supercapacitor cells. Considering the requirement of the above-mentioned system parameter, the supercapacitor array based on several individual supercapacitors cells connected in series or parallel can be established by using the following equation [44]:

$$C_{system} = C_{Cell} \times \frac{Parallel\ Cells}{Series\ Cells}. \tag{9}$$

The equivalent series resistance of the supercapacitor array can be determined as:

$$R_{system} = R_{Cell} \times \frac{Series\ Cells}{Paralle\ lCells}. \tag{10}$$

Equation 9 and 10 have been used to achieve the optimal arrangement and suitable size of supercapacitors, which satisfy the system parameters requirements.

VI. SIMULATION AND EXPERIMENTAL RESULTS

A. SIMULATION TEST SET-UP AND RESULTS

The simulations of the proposed WECS are conducted in Proteus software by Labcenter Electronics. Figure 8 shows the sub-circuits of WECS, that is, the wind turbine mimicking converter, supercapacitor module, and charge controller connected in the simulation environment.

At the first stage, the mimicking converter obtains wind profile data from a pre-defined look-up table programmed

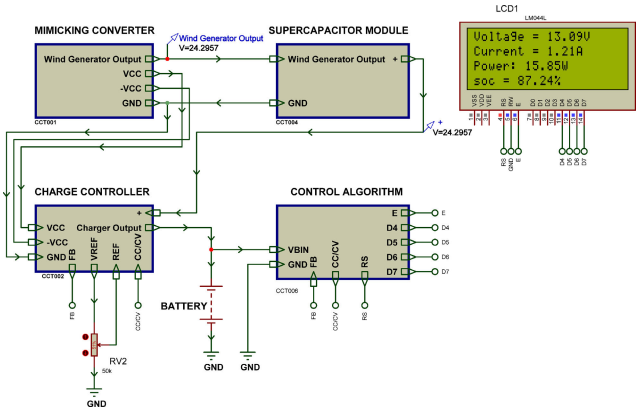

FIGURE 8. Sub-circuits of the WECS in proteus simulation software.

in a microcontroller. Owing to variable wind speed data, the output of the converter is variable DC voltage. The supercapacitor module is connected to the converter to create a stable output power. The stable output power from the supercapacitor module is fed to the charge controller. The charge controller then charges the battery according to its SOC.

The constant current (CC) mode simulation test of the WECS with conventional and hybrid energy storage are performed independently. Figure 9 shows the graph of battery charging of conventional WECS (with battery storage only) system during CC mode. The charging current continuously changes irrespective of desired current for battery charging. This is due to variable output of the mimicking converter, and as consequence, these current spikes damage the battery.

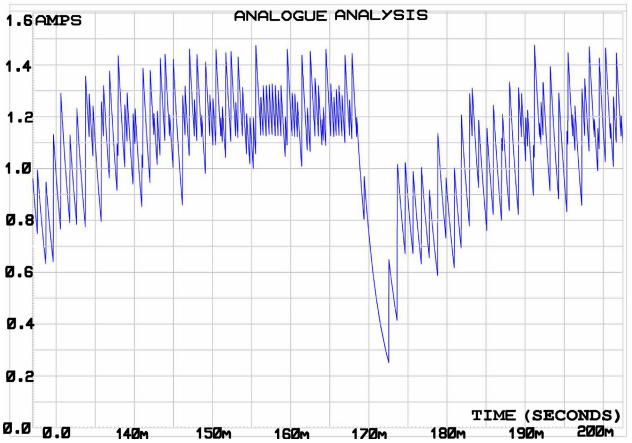

FIGURE 9. Battery charging current of conventional WECS during CC mode.

However, the charging pattern of the WECS with hybrid energy storage system (HESS) indicates that charging current is stable, as shown in Figure 10. Compared with the conventional system, the charging pattern of hybrid energy storage will increase battery lifetime due to stable output power supplied to the battery.

The behavior for both WECS systems in simulation environment is tested for constant voltage mode.

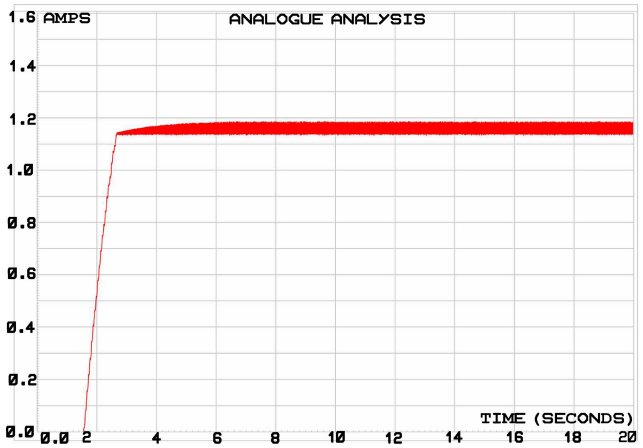

FIGURE 10. Battery charging current of proposed WECS during CC mode.

Figure 11 shows the variable output current in case of conventional system, where the current varies between 3.8 A to 0.3 A. However, when the circuit with integrated supercapacitor module is tested during CV mode, it shows a gradual decline of current as the battery gets charged with the time. The Figure 12 depicts the behavior of proposed system during CV mode.

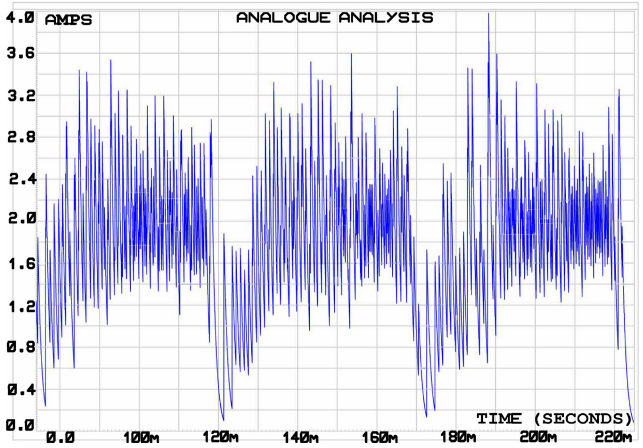

FIGURE 11. Battery charging current of conventional WECS during CV Mode.

B. EXPERIMENTAL TEST SET-UP AND RESULTS

A prototype of the proposed WECS is constructed using available resources in the laboratory. The test bench set-up includes regulated DC power supplies, specialized wind turbine mimicking converter, data-logging board, supercapacitors, charge controller, and batteries. The specialized converter is assigned with real-time data of the wind energy in the localized area. This special purpose-built converter is used to provide a variable output voltage to the supercapacitor to mimic the power fluctuations produced by the wind turbine in real time. However, the customized design of the converter is beyond the scope of this research. The data- logging

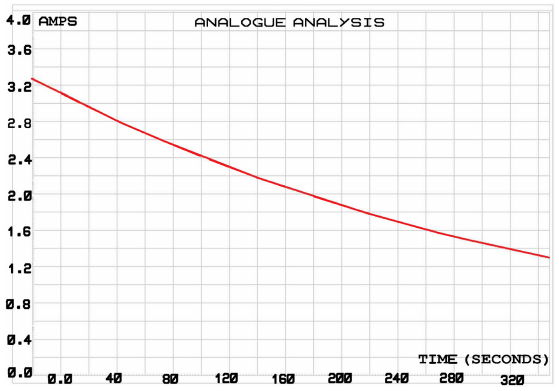

FIGURE 12. battery charging current of proposed WECS during CV Mode.

board is developed to assess the performance of the proposed WECS and to ensure the implementation of the localized wind energy profile. By using the sizing principle mentioned above, an array of supercapacitors is created. It consists of nine series-connected cells, each rated 2.7 Vdc, 500 F, and generates a total nominal voltage of 24.3 V DC and 55.5 F, as shown in Figure 13.

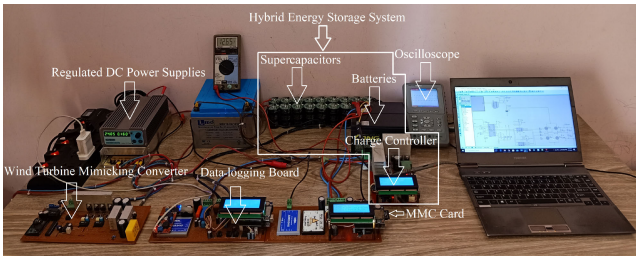

FIGURE 13. Experimental set-up of wind energy conversion system.

To control the switching of the DC-DC converter, DC charge controller, the IRF1404 MOSFET from *International Rectifier* is used. Battery current (I_{bat}) and voltage (V_{bat}) are measured using the LEM current transducer (LAH-25).

The charge controller is connected with the supercapacitor module, as depicted in experimental set-up shown in Figure 13. This converter is used to charge the battery. The charging control algorithm is implemented using industrial-grade microcontroller ATmega328 to charge the battery in CC and constant voltage (CV) mode. The real-time clock DS1307 module, which is connected to the microcontroller, is used for data-logging purposes to record power variations produced by the specialized converter. To validate the proposed control scheme, the CC was set to $I_{bat} = 1.4$ A. During the CC mode, the battery charging current remains constant until the terminal voltage of the battery reaches 13.5 V. The charge control algorithm switches to CV mode as its condition is satisfied. During the CV mode, the battery terminal voltage is set to a constant 14 V, and the battery current is gradually reduced to 0.1 A. The battery voltage increases to 14.4 V. Figure 14 illustrates the constant current charging

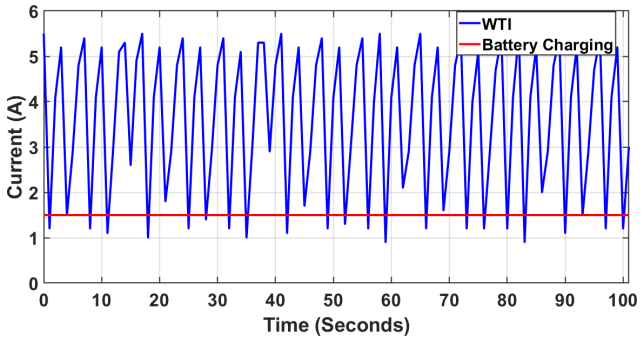

FIGURE 14. Constant current charging of proposed system.

mode. The current from the wind turbine pulsates between 5 A and 2 A, whereas the output of the supercapacitor is held constant at 1.4 A.

Figure 15 shows the output current of the wind turbine and supercapacitor during CV mode. The wind turbine current pulsates between 5 A to 1 A, whereas the output current of the supercapacitor gradually decreases as described above in the section of the control algorithm.

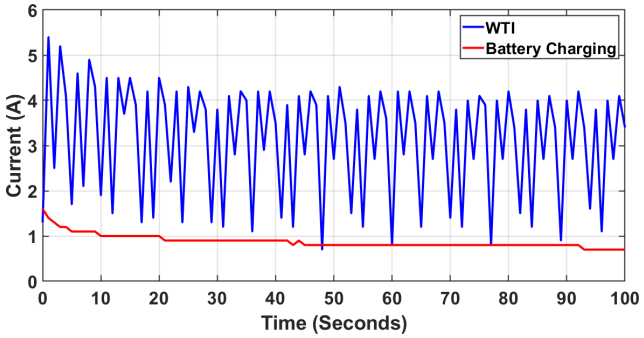

FIGURE 15. Constant voltage charging of proposed system.

To compare the performance of the proposed system with the conventional method of charging, the supercapacitor module was disconnected from the WECS system for tests. The results were analyzed during CC and CV mode, and significant oscillations were recorded in the absence of a supercapacitor. Figure 16 shows that the wind turbine current and battery current, which is the output of DC charge controller, were continuously changing even if the current set point is fixed to 1.4 A.

The same behavior can be observed in Figure 17 in the CV mode. In the absence of a supercapacitor, both output currents kept oscillating. Such fluctuations reduce the efficiency of the WECS and battery life as well.

To assess the performance of the proposed WECS system, few charge and discharge tests were conducted and compared with the test results of the conventional system. Figures 18 and 19 represent the V/Amp–time characteristics of the battery in WECS with HESS and conventional systems during charging respectively. The battery terminal threshold voltage was kept at 12.48 V at the start of the charging

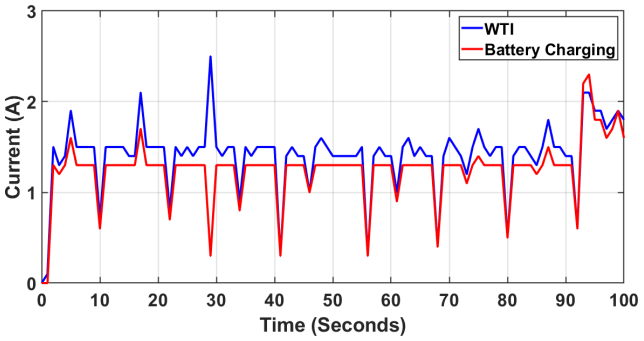

FIGURE 16. Constant current charging of conventional system.

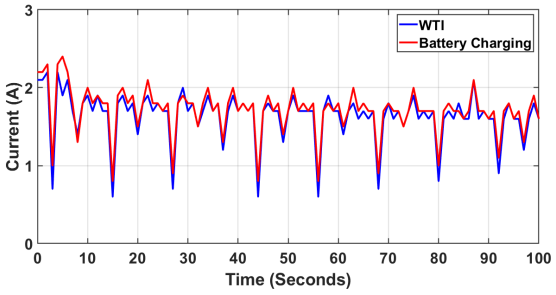

FIGURE 17. Constant voltage charging of conventional system.

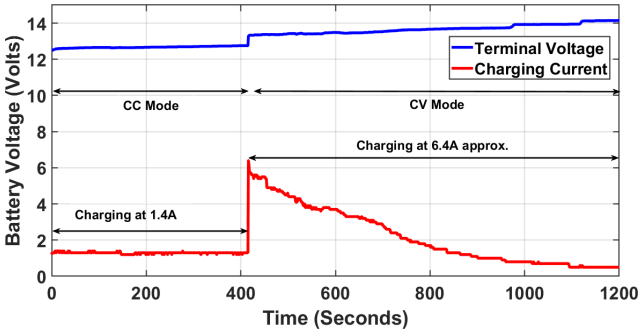

FIGURE 18. Battery charging cycle of proposed system.

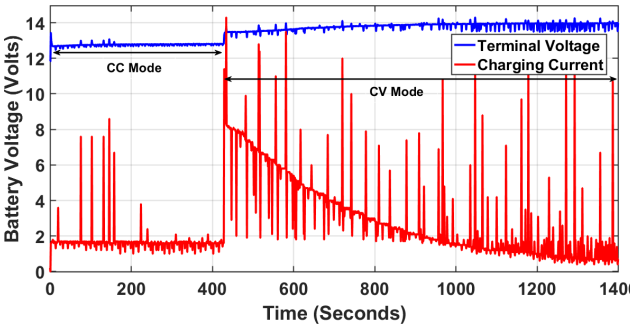

FIGURE 19. Battery charging cycle of conventional system.

process. At the first stage, which is constant current mode, the charge rate C/10 current was controlled until the terminal voltage of the battery reached 13.5 V. However, in the second stage, the voltage was only a controlled parameter.

The results indicate that the peak current in the case of WECS with a hybrid energy storage system is considerably less than that in the conventional WECS. By contrast, in WECS without a supercapacitor, current varies continuously to an unsafe level, as shown in Figure 19. Given that the current is not controlled during CV mode, the current in battery terminals pulsates significantly high.

The rise in current produces stress in the battery and reduces its lifetime [13]. The figures above indicate that the battery current maxima can be eliminated effectively with the integration of a supercapacitor in WECS.

A voltage profile of the battery charging of WECS integrated with a supercapacitor is compared with the conventional WECS system in Figure 20. The lower threshold voltage and upper threshold voltages are predefined as 10 V and 14.4 V, respectively, for both cases.

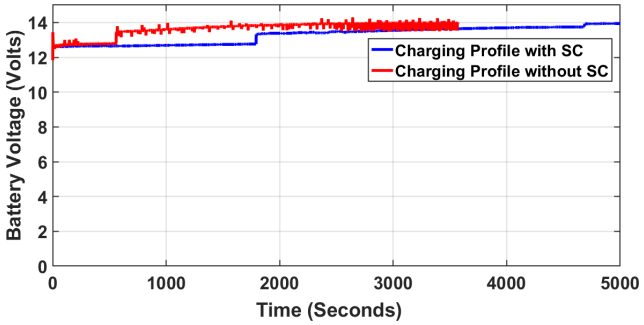

FIGURE 20. Comparison of battery charging profiles of proposed system and conventional system.

The battery of the WECS without a supercapacitor is charged faster than the battery of the WECS with a supercapacitor.

This difference is because of irregular current peaks arising during the CV mode, which causes the battery cells to reach gassing voltage quickly.

However, these current peaks charge the battery rapidly but also surpass the gassing voltage of cells. When the battery exceeds the nominal gassing voltage, gases can flee from the safety valves, thereby reducing battery lifetime [45].

Moreover, the SOC of battery is high in CV mode. These current peaks also occur in this mode, because high SOC of a battery presents high resistance to charge acceptance and causes heat losses due to these current peaks [38].

Figure 21 compares the voltage profiles of the battery of WECS charged with and without a supercapacitor. The discharge profile for the 12 V lead–acid battery was used for the experiment. The tests were conducted using a resistive load of 8Ω at the C/8 discharge rate. The initial voltage at the battery terminals was 12.95 V in both cases. The battery of the WECS without a supercapacitor is discharged faster than the battery of the WECS integrated with a supercapacitor. Batteries have a considerable impact on overall system performance, which also affects the efficiency of the power conversion system [36].

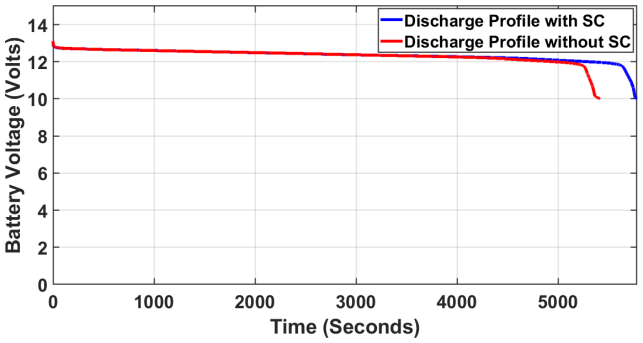

FIGURE 21. Comparison of battery discharge profiles between proposed system and conventional system.

To differentiate the performance of WECS with HESS as compared to conventional WECS some key parameters are tabulated in Table 2. In the test set-up, the battery is charged with the SOC from 86 % to 100 %, while, the discharge tests are conducted with the SOC from 90 % to 69.5 %. The deviations in current and voltage during CC and CV modes reflect the robustness of the system against fluctuations. The deviations in current during CC mode are negligible in proposed system while the current in conventional system varies between 1.2 A to 8.7 A. During the CV mode, the current deviation is approximately twice in conventional system as compared to proposed system. The voltage deviations in WECS with HESS is as half as in the conventional system during CC mode, however, the voltage does not vary significantly during CV mode in both systems. Due to high power injection in conventional system the battery takes significantly less time than in proposed system. But this charging pattern in conventional system dissipates the battery power in a short time despite of same load being used for discharging in both the systems. This decreases the battery lifecycles in conventional system and consequently the battery lifetime will be reduced. When the charging and discharging time of the both systems are compared, it can be realized that the integration of supercapacitor increases the battery lifetime and it also improves efficiency of the system by withstanding the power fluctuations.

In addition to the assessment of the battery charging/discharging behavior, it is also important to monitor the responses of parameters of wind turbine generator. For this purpose, a test bench is developed, as shown in Figure 22, which includes wind turbine PMSG, voltage/current measurement circuit, three-phase rectifier, supercapacitor module, charge controller and battery. Different tests have been performed to track some of the parameters of the wind turbine generator like terminal voltage, terminal current, reactive power response and DC-link voltage of the charge controller. The wind turbine generator is delta (Δ) connected and the output terminals are passed through the current transducer LAH-50 for current measurement. The current and voltage are measured using GW Instek oscilloscope. The output from current transducer is fed to three-phase rectifier which supplies power to supercapacitor module. The stored DC

TABLE 2. Performance evaluation of convensional system and WECS with HESS.

Method	Conventional WECS		WECS with HESS	
Charging Mode	CC Mode	CV Mode	CC Mode	CV Mode
SOC (%)	86 to 89	89 to 100	86.6 to 88.6	88.6 to 100
Current deviation (average)	7.5 A	13.9 A	0.2 A	6 A
Voltage deviation (average)	0.43 V	1.06 V	0.18 V	0.98 V
Power fluctuations (average)	15 – 114 (W)	14.1 – 215 (W)	15 – 17.5 (W)	5.7 – 85.2 (W)
Battery Charging Time (SOC 86.6 % to 100 %)	58 minutes	11 minutes	62 minutes	148 minutes
Battery Discharging Time (SOC 89.7 % to 69.5 %)	80 minutes		203 minutes	

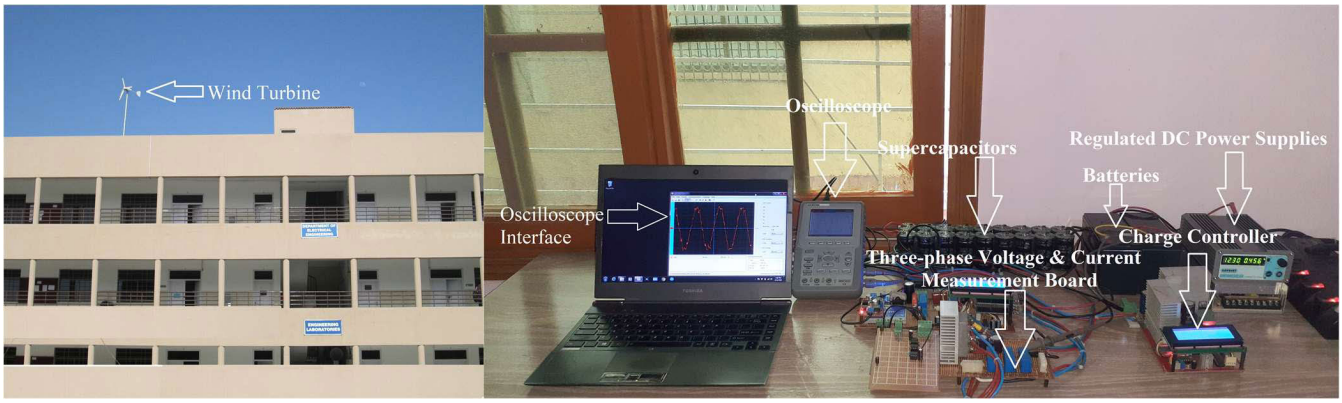

FIGURE 22. Complete test bench set-up of WECS.

power in supercapacitor is fed to charge controller which maintains constant power for battery charging.

The behavior of terminal voltage of PMSG is analyzed for both the proposed WECS with HESS and the conventional system. The measured terminal voltage of conventional system is shown in Figure 23. The voltages are distorted due to nonlinear behavior of diode rectifier. Whereas, in the system with HESS, the quality of terminal voltages is improved as stable power is drawn when the supercapacitor gets fully charged and it can be noticed in Figure 24. The reactive power is observed at the terminals of PMSG. When the power is fed to the rectifier in case of conventional WECS and the charge controller starts the charging of battery. Due to link capacitor and battery the current leads the voltage as shown in Figure 25. Due to variable output of wind turbine generator, the waveforms are distorted in conventional system. However, it can be observed in the WECS with HESS, the supercapacitor maintains constant power supply to DC-link, and it causes improvement in power factor at PMSG terminals.

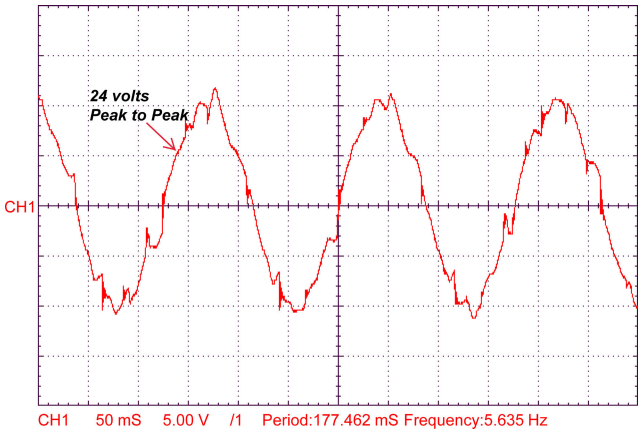

FIGURE 23. Generator terminal voltage in conventional system.

Moreover, the effect of variable output of wind turbine is countered by the supercapacitor and the waveforms are improved when compared to conventional system as shown in Figures 26.

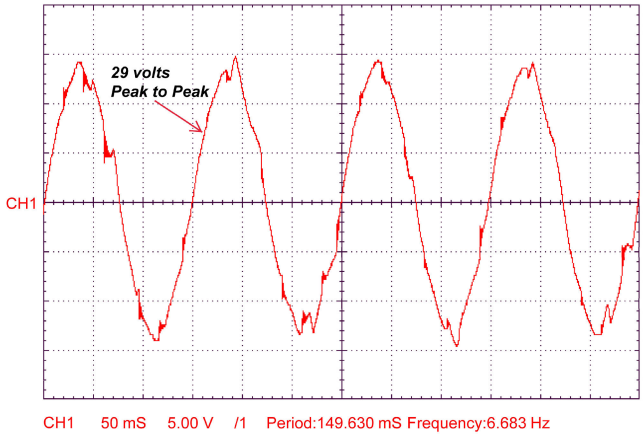

FIGURE 24. Generator terminal voltage in proposed system.

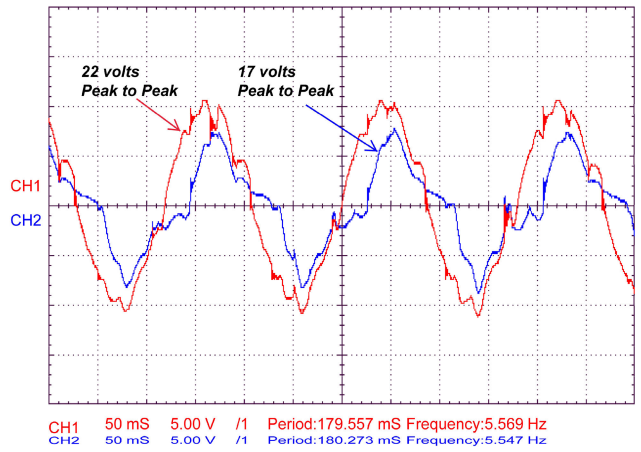

FIGURE 25. Reactive power (V, I) in conventional system.

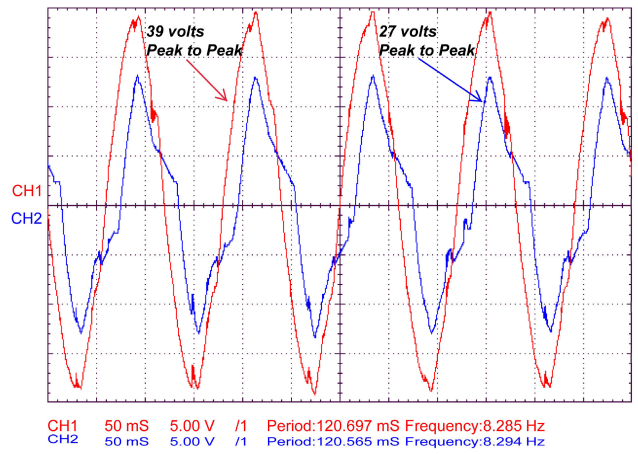

FIGURE 26. Reactive power (V, I) in proposed system with fully charged supercapacitor.

The DC-link voltage in conventional WECS system is measured and shown in Figure 27. Although the output of PMSG varies with respect to windspeed but it is difficult to measure and show the real time changes of DC-link voltage

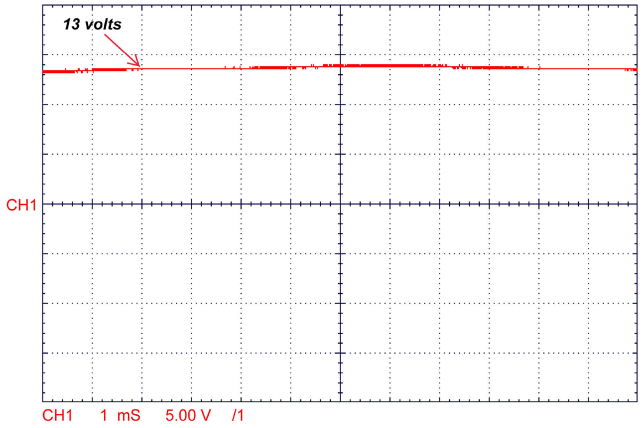

FIGURE 27. DC-Link voltage in conventional system.

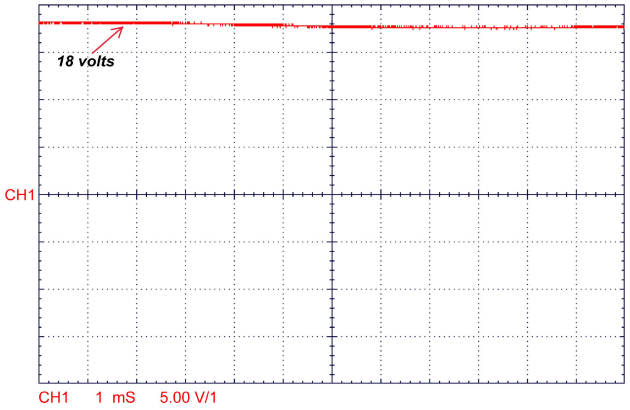

FIGURE 28. DC-Link voltage in proposed system.

on oscilloscope. A disturbance ramp of fractional value in DC-link voltage can be observed. Whereas, in WECS with HESS, the DC-link voltage is maintained due to integration of supercapacitor and the voltage remains constant at 18 V as shown in Figure 28. The maintained DC-link voltage helps to reduce the stress on the switches of charge controller and increases the efficiency of system.

VII. CONCLUSION

This research presents the application of a supercapacitor in WECS to increase the life of the lead–acid battery. The study illustrates the significant improvement in battery lifetime by integrating a supercapacitor in the proposed WECS, which eliminates power fluctuations caused by variable wind speed and instantaneous load switching. Several simulation and experimental tests were conducted on proposed and conventional WECS to highlight the improvement in battery life. Wind data of localized area are incorporated in a special purpose-built converter, which produces actual wind energy and power fluctuations recorded in real-time. The experimental results indicate that current spikes range to an unsafe level in the conventional system. These current variations cause enormous stress on the battery by increasing the voltage

of cells. Furthermore, the study shows that the battery of a conventional system is charged faster than the proposed system, but it also discharges earlier due to the penetration of high current in the battery during the CV mode of charging in conventional WECS. Current oscillations produce heat loss and consequently reduce the efficiency of battery and overall system. The behavior of wind turbine generator variables is tested on an additional set-up and the results indicate improvement in DC-link, terminal voltage, and reactive power. Thus, the integration of a supercapacitor provides a smooth charging and extended discharging of the battery and keeps the power electronic circuit safe from current spikes during the charging cycles of battery. Moreover, the improvement in wind turbine generator variables causes reduced stress on the generator and ancillary components of the circuit.

REFERENCES

[1] B. Yu, "Design and experimental results of battery charging system for microgrid system," *Int. J. Photoenergy*, vol. 2016, pp. 1–6, Jan. 2016.

[2] A. H. Chowdhury, "Design strategy for an off-grid solar-wind hybrid power system," Dept. Elect. Electron. Eng., Bangladesh Univ. Eng. Technol., Dhaka, Bangladesh, Tech. Rep., 2014.

[3] P. S. Kumar, R. P. S. Chandrasena, V. Ramu, G. N. Srinivas, and K. V. S. M. Babu, "Energy management system for small scale hybrid wind solar battery based microgrid," *IEEE Access*, vol. 8, pp. 8336–8345, 2020.

[4] F. Díaz-González, A. Sumper, O. Gomis-Bellmunt, and R. Villafáfila-Robles, "A review of energy storage technologies for wind power applications," *Renew. Sustain. Energy Rev.*, vol. 16, no. 4, pp. 2154–2171, May 2012.

[5] F.-B. Wu, B. Yang, and J.-L. Ye, *Grid-Scale Energy Storage Systems and Applications*. New York, NY, USA: Academic, 2019.

[6] S. K. Kollimalla, M. K. Mishra, and N. L. Narasamma, "Design and analysis of novel control strategy for battery and supercapacitor storage system," *IEEE Trans. Sustain. Energy*, vol. 5, no. 4, pp. 1137–1144, Oct. 2014.

[7] R. Sathishkumar, S. K. Kollimalla, and M. K. Mishra, "Dynamic energy management of micro grids using battery super capacitor combined storage," in *Proc. Annu. IEEE India Conf. (INDICON)*, Dec. 2012, pp. 1078–1083.

[8] L. Li, Z. Huang, H. Li, and H. Lu, "A high-efficiency voltage equalization scheme for supercapacitor energy storage system in renewable generation applications," *Sustainability*, vol. 8, no. 6, p. 548, Jun. 2016.

[9] M. Bayya, U. M. Rao, B. P. Rao, and N. M. Muthukrishnan, "Comparison of voltage charging techniques to increase the life of lead acid batteries," in *Proc. IEEE Int. Symp. Smart Electron. Syst. (iSES) (Formerly iNiS)*, Dec. 2018, pp. 279–284.

[10] A. M. van Voorden, L. M. R. Elizondo, G. C. Paap, J. Verboomen, and L. van der Sluis, "The application of super capacitors to relieve battery-storage systems in autonomous renewable energy systems," in *Proc. IEEE Lausanne Power Tech*, Jul. 2007, pp. 479–484.

[11] T. Wen, Z. Zhang, X. Lin, Z. Li, C. Chen, and Z. Wang, "Research on modeling and the operation strategy of a hydrogen-battery hybrid energy storage system for flexible wind farm grid-connection," *IEEE Access*, vol. 8, pp. 79347–79356, 2020.

[12] A. M. Gee and R. W. Dunn, "Novel battery/supercapacitor hybrid energy storage control strategy for battery life extension in isolated wind energy conversion systems," in *Proc. 45th Int. Universities Power Eng. Conf. (UPEC)*, Aug. 2010, pp. 1–6.

[13] A. M. Gee, F. V. P. Robinson, and R. W. Dunn, "Analysis of battery lifetime extension in a small-scale wind-energy system using supercapacitors," *IEEE Trans. Energy Convers.*, vol. 28, no. 1, pp. 24–33, Mar. 2013.

[14] Q. Jiang, Y. Gong, and H. Wang, "A battery energy storage system dual-layer control strategy for mitigating wind farm fluctuations," *IEEE Trans. Power Syst.*, vol. 28, no. 3, pp. 3263–3273, Aug. 2013.

[15] T. R. Ayodele, A. S. O. Ogunjuyigbe, and B. E. Olateju, "Improving battery lifetime and reducing life cycle cost of a PV/battery system using supercapacitor for remote agricultural farm power application," *J. Renew. Sustain. Energy*, vol. 10, no. 1, Jan. 2018, Art. no. 013503.

[16] W. Jing, C. Hung Lai, S. H. W. Wong, and M. L. D. Wong, "Battery-supercapacitor hybrid energy storage system in standalone DC microgrids: Areview," *IET Renew. Power Gener.*, vol. 11, no. 4, pp. 461–469, Mar. 2017.

[17] B. Luo, D. Ye, and L. Wang, "Recent progress on integrated energy conversion and storage systems," *Adv. Sci.*, vol. 4, no. 9, Sep. 2017, Art. no. 1700104.

[18] S. Yushu, Z. Zhenxing, Y. Min, J. Dongqiang, P. Wei, and X. Bin, "Research overview of energy storage in renewable energy power fluctuation mitigation," *CSEE J. Power Energy Syst.*, vol. 6, no. 1, pp. 160–173, 2019.

[19] M. Khalid, "A review on the selected applications of battery-supercapacitor hybrid energy storage systems for microgrids," *Energies*, vol. 12, no. 23, p. 4559, Nov. 2019.

[20] V. Jülch, "Comparison of electricity storage options using levelized cost of storage (LCOS) method," *Appl. Energy*, vol. 183, pp. 1594–1606, Dec. 2016.

[21] W. Jing, C. H. Lai, W. S. H. Wong, and M. L. D. Wong, "A comprehensive study of battery-supercapacitor hybrid energy storage system for standalone PV power system in rural electrification," *Appl. Energy*, vol. 224, pp. 340–356, Aug. 2018.

[22] W. Zuo, R. Li, C. Zhou, Y. Li, J. Xia, and J. Liu, "Battery-supercapacitor hybrid devices: Recent progress and future prospects," *Adv. Sci.*, vol. 4, no. 7, Jul. 2017, Art. no. 1600539.

[23] N. R. Babu and P. Arulmozhivarman, "Wind energy conversion systems-a technical review," *J. Eng. Sci. Technol.*, vol. 8, no. 4, pp. 493–507, 2013.

[24] L. H. Hansen, P. H. Madsen, F. Blaabjerg, H. C. Christensen, U. Lindhard, and K. Eskildsen, "Generators and power electronics technology for wind turbines," in *Proc. 27th Annu. Conf. IEEE Ind. Electron. Soc.*, vol. 3, Nov. 2001, pp. 2000–2005.

[25] L. H. Hansen, L. Helle, F. Blaabjerg, E. Ritchie, S. Munk-Nielsen, H. W. Bindner, P. E. Sørensen, and B. Bak-Jensen, "Conceptual survey of generators and power electronics for wind turbines," Forskningscenter Risoe, Roskilde, Denmark, Risoe-R 1205(EN), 2002.

[26] T. Kanda, L. P. Mdakane, C. J. J. Labuschagne, and M. J. Kamper, "Dynamics of maximum power point wind energy battery charging systems," in *Proc. Southern Afr. Univ. Power Eng. Conf./Robot. Mechatronics/Pattern Recognit. Assoc. South Afr. (SAUPEC/RobMech/PRASA)*, Jan. 2019, pp. 576–581.

[27] S. Nallusamy, D. Velayutham, and U. Govindarajan, "Design and implementation of a linear quadratic regulator controlled active power conditioner for effective source utilisation and voltage regulation in low-power wind energy conversion systems," *IET Power Electron.*, vol. 8, no. 11, pp. 2145–2155, Nov. 2015.

[28] J. F. Manwell, J. G. McGowan, and A. L. Rogers, *Wind Energy Explained: Theory, Design and Application*. Hoboken, NJ, USA: Wiley, 2010.

[29] G. L. Johnson, *Wind Energy Systems*. Upper Saddle River, NJ, USA: Prentice-Hall, 1985.

[30] D. Ciarlini Chagas Freitas, J. Lopes de Moraes, E. Cavalcanti Neto, and J. R. B. Sousa, "Battery charger lead-acid using IC BQ2031," *IEEE Latin Amer. Trans.*, vol. 14, no. 1, pp. 32–37, Jan. 2016.

[31] T. Szepesi, "Stabilizing the frequency of hysteretic current-mode DC/DC converters," *IEEE Trans. Power Electron.*, vol. PE-2, no. 4, pp. 302–312, Oct. 1987.

[32] *Regulating Pulse Width Modulators*, Texas Instrum., Dallas, TX, USA, Jan. 2008.

[33] H. Keshan, J. Thornburg, and T. S. Ustun, "Comparison of lead-acid and lithium ion batteries for stationary storage in off-grid energy systems," Dept. Elect. Eng., PEC Univ. Technol., Chandigarh India, Tech. Rep., 2016.

[34] K.-S. Ng, C.-S. Moo, Y.-P. Chen, and Y.-C. Hsieh, "State-of-charge estimation for lead-acid batteries based on dynamic open-circuit voltage," in *Proc. IEEE 2nd Int. Power Energy Conf.*, Dec. 2008, pp. 972–976.

[35] E. Kurniawan, B. Rahmat, T. Mulyana, and J. Alhilman, "Data analysis of li-ion and lead acid batteries discharge parameters with simulink-MATLAB," in *Proc. 4th Int. Conf. Inf. Commun. Technol. (ICoICT)*, May 2016, pp. 1–5.

[36] H. Bindner, T. Cronin, P. Lundsager, J. F. Manwell, U. Abdulwahid, and I. Baring-Gould, "Lifetime modelling of lead acid batteries," Risø Nat. Lab., Roskilde, Denmark, Tech. Rep. Risø-R-1515(EN), 2005.

[37] H. A. Serhan and E. M. Ahmed, "Effect of the different charging techniques on battery life-time: Review," in *Proc. Int. Conf. Innov. Trends Comput. Eng. (ITCE)*, Feb. 2018, pp. 421–426.

[38] H. Fakham, D. Lu, and B. Francois, "Power control design of a battery charger in a hybrid active PV generator for load-following applications," *IEEE Trans. Ind. Electron.*, vol. 58, no. 1, pp. 85–94, Jan. 2011.

[39] T. Morgan, "Guide to charging sealed lead acid batteries," tehnična dokumentacija, Silver Telecom Ltd., Newport, Wales, Tech. Rep., 2014.
[40] J. B. Ekanayake, N. Jenkins, K. Liyanage, J. Wu, and A. Yokoyama, *Smart Grid: Technology and Applications*. Hoboken, NJ, USA: Wiley, 2012.
[41] M. A. Guerrero, E. Romero, F. Barrero, M. I. Milanés, and E. Gonzalez, "Supercapacitors: Alternative energy storage systems," *Przegląd Elektrotechniczny*, vol. 85, no. 10, pp. 188–195, 2009.
[42] L. Zubieta and R. Bonert, "Characterization of double-layer capacitors for power electronics applications," *IEEE Trans. Ind. Appl.*, vol. 36, no. 1, pp. 199–205, Jan. 2000.
[43] N. Gekakis, A. Nadeau, M. Hassanalieragh, Y. Chen, Z. Liu, G. Honan, F. Erdem, G. Sharma, and T. Soyata, "Modeling of supercapacitors as an energy buffer for cyber-physical systems," in *Cyber-Physical Systems: A Computational Perspective*. Milton Park, U.K.: Taylor & Francis, 2015, pp. 171–189.
[44] D. Petreus, D. Moga, R. Galatus, and R. A. Munteanu, "Modeling and sizing of supercapacitors," *Adv. Electr. Comput. Eng.*, vol. 8, no. 2, pp. 15–22, 2008.
[45] K. C. Tseng, T. J. Liang, J. F. Chen, and M. T. Chang, "High frequency positive/negative pulse charger with power factor correction," in *Proc. IEEE 33rd Annu. IEEE Power Electron. Spec. Conf.*, vol. 2, Jun. 2002, pp. 671–675.

IRFAN HUSSAIN PANHWAR received the B.S. degree in electronics engineering and the M.S. degree in electrical power engineering. He was an Electronic Design Engineer with Ibn Khaldun Systems, Karachi, Pakistan. He has designed power converters for renewable energy systems. He is currently the Laboratory Instructor with the Electrical Engineering Department, DHA Suffa University, Karachi. His research interests include the design of high-end power converters for renewable energy systems and battery lifetime extension using sophisticated charge techniques.

KAFEEL AHMED (Member, IEEE) received the B.Eng. degree in electrical power engineering and the M.Eng. degree in electrical engineering. He is currently pursuing the Ph.D. degree with the School of Software and Electrical Engineering, Swinburne University of Technology, Melbourne, VIC, Australia.

Prior to his Ph.D. studies, he was a Senior Lecturer with DHA Suffa University, Karachi, Pakistan. His research interests include renewable energy systems, micro-grid systems, wireless power transfer, and power conversion.

MEHDI SEYEDMAHMOUDIAN (Member, IEEE) received the B.Sc. degree in electrical power engineering, the M.Eng. degree in industrial control and electronic, and the Ph.D. degree in electrical engineering. He was a Lecturer and a Course Coordinator with the School of Engineering, Deakin University, Geelong, VIC, Australia. He is currently a Senior Lecturer with the School of Software and Electrical Engineering, Swinburne University of Technology, Melbourne, VIC, Australia. His research interests include renewable energy systems, smart grids and micro-grid systems, and the application of emerging technologies in green renewable energy development.

ALEX STOJCEVSKI (Senior Member, IEEE) received the bachelor's degree in electrical engineering, the master's degree in electrical and electronics engineering, the master's degree in education and project-based learning in engineering and science from Aalborg University, Denmark, and the D.Phil. degree. He has held numerous senior positions in several universities across different countries. His research interests include renewable energy and micro-grid design. He has published more than 250 book chapters, journals, and conference papers and has given a number of international presentations as an invited speaker.

BEN HORAN (Member, IEEE) received the B.Eng. (Hons.) and Ph.D. degrees in engineering from Deakin University, Geelong, VIC, Australia, in 2005 and 2009, respectively. He is currently an Associate Professor and the Associate Head of the School-Research and the Director of the CADET VR Lab, School of Engineering, Deakin University. His research interests include mechatronics, virtual reality, and renewable energy.

SAAD MEKHILEF (Senior Member, IEEE) is currently a Professor with the Department of Electrical Engineering, University of Malaya, Malaysia. He is also the Director of the Power Electronics and Renewable Energy Research Laboratory (PEARL). He is the author or coauthor of more than 250 publications in international journals and proceedings. He is actively involved in industrial consultancy for major corporations in power electronics projects. His research interests include power conversion techniques, control of power converters, renewable energy, and energy efficiency. He is an IET Fellow. He is the Associate Editor of IEEE TRANSACTIONS ON POWER ELECTRONICS and *Journal of Power Electronics*.

ASIM ASLAM received the bachelor's degree in electrical engineering from DHA Suffa University in 2018. He holds in-depth knowledge and significant experience in the design, installation, and maintenance of various renewable energy systems. His research interests include grid interaction studies and development of advance power converters for solar and wind farms.

MARYAM ASGHAR (Member, IEEE) was born in Karachi, Pakistan, in 1998. She received the bachelor's degree from DHA Suffa University in 2019. She graduated as an Electrical Engineer with Power Systems as her major. Her interests include renewable energy sources, their control systems, and the power electronics involved. Her research interests include AI and robotic systems.